Kynurenamines as Neural Nitric Oxide Synthase Inhibitors

Antonio Entrena,[†] M. Encarnación Camacho,[†] M. Dora Carrión,[†] Luisa C. López-Cara,[†] Guillermo Velasco,[†] Josefa León,[‡] Germaine Escames,[‡] Darío Acuña-Castroviejo,[‡] Víctor Tapias,[‡] Miguel A. Gallo,[†] Antonio Vivó,[§] and Antonio Espinosa*,[†]

Departamento de Química Farmacéutica y Orgánica, Facultad de Farmacia, Universidad de Granada, 18071 Granada, Spain, Departamento de Fisiología, Instituto de Biotecnología, Universidad de Granada, 18071 Granada, Spain, and Hospital Costal del Sol, Marbella (Málaga), Spain

To find new compounds with potential neuroprotective activity, we have designed, synthesized, and characterized a series of neural nitric oxide synthase (nNOS) inhibitors with a kynurenamine structure. Among them, *N*-[3-(2-amino-5-methoxyphenyl)-3-oxopropyl]acetamide is the main melatonin metabolite in the brain and shows the highest activity in the series, with an inhibition percentage of 65% at a 1 mM concentration. The structure−activity relationship of the new series partially reflects that of the previously reported 2-acylamido-4-(2-amino-5-methoxyphenyl)-4-oxobutyric acids, endowed with a kynurenine-like structure. Structural comparisons between these new kinurenamine derivatives, kynurenines, and 1-acyl-3-(2-amino-5-methoxyphenyl)-4,5-dihydro-1*H*-pyrazole derivatives also reported confirm our previous model for the nNOS inhibition.

Introduction

N-methyl-D-aspartate (NMDA) receptors are a subtype of receptors that, activated by glutamate, gather the influx of Ca^{2+} into the neuronal cell, along with a flux of other ions such as Na^+ and K^+.[1] An overstimulation of the NMDA receptors produces an accumulation of intracellular Ca^{2+} that, in turn, activates a series of enzymes such as lipases, proteases, and nitric oxide synthase (NOS), thus leading to the formation of reactive oxygen species (ROS), responsible for the neuronal damage.[2−4]

Nitric oxide (NO) is a well-known biologically active compound that acts as a cell messenger with important regulatory functions in the nervous, immune, and cardiovascular systems.[5] In mammals, NO is synthesized from L-arginine in various cell types (neurons,[6] endothelial cells,[7] and macrophages[8,9]) by a family of nitric oxide synthase (NOS) isoenzymes.[10,11] The constitutive endothelial (eNOS) and neural (nNOS) isoforms are calcium/calmodulin dependent and are physiologically activated by hormones or neurotransmitters that increase the intracellular calcium concentration.

In contrast, the inducible (iNOS) isoform is activated by basal intracellular calcium concentrations, and once expressed, it remains permanently activated, yielding high NO concentrations. This mechanism is part of the normal immune response against invading pathogens and neoplastic cells.[12] Although NO is not involved in the synaptic transmission under normal conditions, an excessive NO production by some of the NOS-isoenzymes may be detrimental. Thus, it is well-known that an overproduction of NO produces neurotoxicity, and

this fact has been associated with several neurological disorders such as Alzheimer's disease,[13,14] amyotrophic lateral sclerosis,[15] and Huntington's disease.[16]

For this reason, a recent strategy in the development of successful neuroprotective agents is orientated toward the synthesis of new structures that interfere with some step of the complex chemical signaling system involving NOS, including the inhibition of the enzyme itself. It has been shown that melatonin (**1**), the main compound secreted by the pineal gland, can inhibit the nNOS activity in rat striatum in a dose-dependent manner.[17] As a consequence of the nNOS inhibition, melatonin also inhibits the NMDA-induced excitation,[18] and it has been proven that this neuroprotective action is unrelated to known melatonin receptors.[19]

In the brain, melatonin is metabolized by the action of the indolamine-2,3-dioxygenase (IDO) to afford the N^1-acetyl-N^2-formyl-5-methoxykynurenine (AFMK). This metabolite is further transformed into *N*-acetyl-5-methoxykynurenamine (aMK), and this is one of the more important metabolic pathways of melatonin in mammalians.[20,21] On the other hand, the action of melatonin can be due to one of these metabolites.[22]

Recently, we have synthesized and evaluated a series of kynurenine derivatives of general formulae **2**, showing a significant nNOS inhibitory activity.[23] In these compounds, the side-chain conformational mobility can be restricted by the formation of an intramolecular hydrogen bond between the 2′-NH_2 and the carbonyl group, and as a consequence of this restriction, the kynurenine derivative can mimic the active conformation of melatonin when it interacts with its biological target.[23]

In a more recent paper, we have described the synthesis of a series of 4,5-dihydro-1*H*-pyrazole derivatives of general formula **3** that constitute a new type and potent nNOS inhibitors.[24]
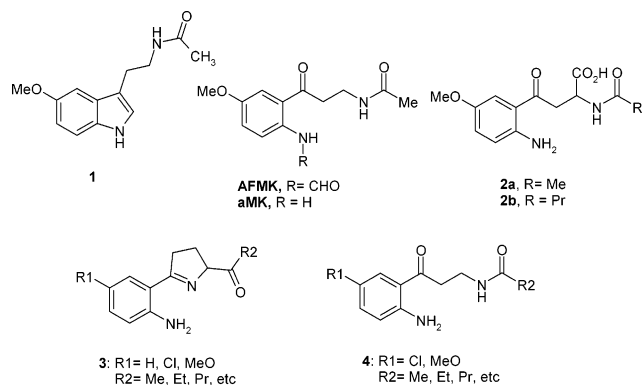
In this paper, we describe the synthesis of a series of kynurenamine derivatives **4**, among which is the

* To whom correspondence should be addressed: Dr. Antonio Espinosa, Departamento de Química Farmacéutica y Orgánica, Facultad de Farmacia, Campus de Cartuja s/n, Universidad de Granada, 18071 Granada (Spain). Phone: +34-958-243850. Fax: +34-958-243845. E-mail: aespinos@ugr.es.
† Departamento de Química Farmacéutica y Orgánica.
‡ Departamento de Fisiología.
§ Hospital Costal del Sol.

1

AFMK, R= CHO
aMK, R = H

2a, R= Me
2b, R = Pr

3: R1= H, Cl, MeO
R2= Me, Et, Pr, etc

4: R1= Cl, MeO
R2= Me, Et, Pr, etc

melatonin metabolite aMK (**4a**, R_1 = OMe, R_2 = Me), that show good nNOS inhibitory activity and could be used as a template in the development of new agents with a neuroprotective mechanism similar to that of melatonin. Due to their similarity with kinurenine, the new kynurenamine derivatives were also tested as inhibitors of the kynurenine 3-hydroxylase (KYN3OH), a key enzyme in the kynurenine pathway, showing that all compounds are inactive against this enzyme.

Chemistry

Scheme 1 represents the general synthetic pathway for all final kynurenamines included in Table 1. 5-Metoxi- and 5-chloro-2-nitrophenyl vinyl ketones **5a** and **5b,** prepared as previously reported[24] from 5-chloro- and 5-hydroxy-2-nitrobenzaldehyde, respectively, were reacted with phthalimide[25] in the presence of NaMeO to afford the intermediates **6a** and **6b** with very high yields (90−92%).

The ketone group of **6a** and **6b** is protected by reaction with ethylene glycol in the presence of *p*-toluenesulfonic acid to yield the dioxolane derivatives **7a−b** (85% in both cases). This protection is necessary because when **6a** or **6b** are directly treated with hydrazine, the phtalimide group opens, and the intermediate hydrazine derivative cyclisizes to afford the intermediate pyrazoline type **8**, which can be converted into the pyrazoline derivative **3** in several steps.[24]

The reaction of **7a** and **7b** with hydrazine opens the phthalimide moiety, and further acidification (HCl) of the reaction mixture allows the hydrolysis of the dioxolane group to yield the corresponding β-aminoketones **9a** and **9b**, which were not isolated. Acylation in situ of **9a** and **9b** by reaction with acetic anhydride or with the corresponding acyl chloride gives rise to the 2′-NO2 derivatives **10a−l**. Yields vary from 70 to 90% in all compounds.

Finally, the reduction of the 2′-NO2 groups in **10a−l** allows for the preparation of the corresponding kynurenamine derivative **4a−l**. This reduction was accomplished by catalytic hydrogenation (H2, Pd/C) in **10a−i** (quantitative yield) and by reaction with Fe/FeSO4 in **10j−l** (95%) to avoid dechlorination.

Results and Discussion

Table 1 and Figure 1 illustrate the nNOS inhibition in the presence of a 1 mM concentration of each kynurenamine **4**. All compounds show good nNOS inhibition, depending on the substitution on both R1 and R2 groups. The influence of R2 on the activity seems to

Scheme 1
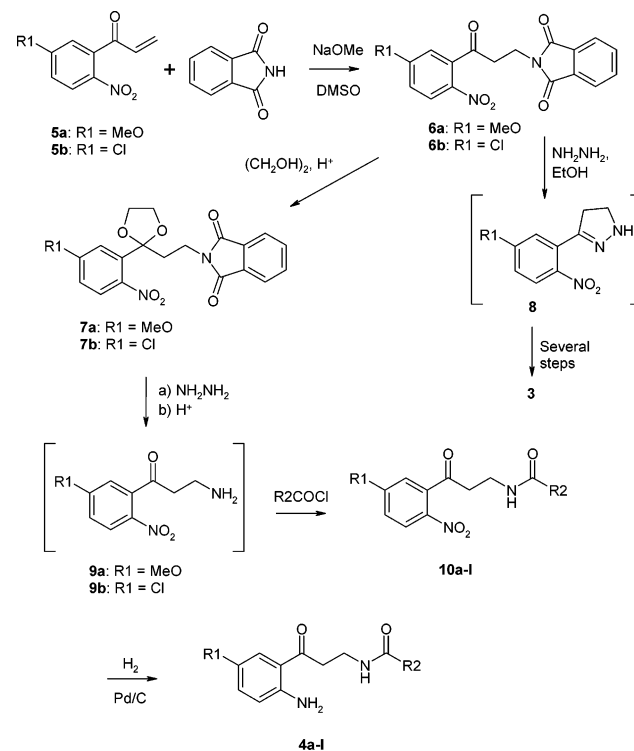
be clear because, in general, it can be observed that an increment in the volume of R_2 decreases the inhibitory activity. Thus, the change of the Me group by Et, Pr, or Bu decreases steadily the percentage of inhibition. The insertion of a cyclopropyl or a phenyl group in R_2 is also detrimental for the activity. In relation to R_1, it can be observed that compounds with R_1 = OMe are about 2 times more active than the corresponding ones with R_1 = Cl, indicating that an electron-withdrawing substituent is detrimental for the activity. Unfortunately, we have not found any quantitative relationships between the volume of the substituent R_2 or the nature of R_1 and the inhibitory activity.

Table 1 and Figure 1 also illustrate the activity of compounds type **4** against KYN3OH. The inhibition of this enzyme has been proposed as a potentially useful strategy for neuroprotection[26] because KYN3OH inhibitors decrease the brain concentration of the neurotoxic quinolinic acid and 3-hydroxykynurenine while increasing the biosynthesis of the neuroprotective kynurenic acid. It can be observed that none of the new compounds showed a significant effect on this enzyme.

In a previous paper,[23] we have described the effects of several kynurenine derivatives of general structure **2** on the excitatory response of striatal neurons to sensorimotor cortex (SMCx) stimulation, an experimental paradigm involving the activation of the NMDA subtype of glutamatergic receptor. Among these compounds, two of them (**2a**, R = Me, and **2b**, R = Pr) showed a strong inhibitory effect on the striatal excitation. Our previous results indicated that there was no response when these compounds were iontophoretized onto a silent neuron in the absence of a NMDA ejection,[23] thus suggesting that they act by reducing the excitatory response elicited by NMDA activation. **2a** and **2b** are also able to significantly reduce the nNOS activity.[23]

Table 1. Structure and Biological Activities of Kynurenamines **4a−l** as nNOS and KYN3OH Inhibitors. Biological Activity of Kinurenines **2** and Pyrazoline **3** Are also Included for Comparison

cmpd	R_1	R_2	% nNOS inhibition[a]	% kynurenine 3-hydroxylase activity[b]
2a	OCH_3	Me	68.49 ± 9.92[c]	100.52 ± 9.7[d]
2b	OCH_3	Pr	45.05 ± 8.56[c]	88.72 ± 10.2[d]
3a	OCH_3	Me	38.04 ± 1.53[d]	98.84 ± 11.3[d]
3b	OCH_3	Et	53.27 ± 2.83[d]	81.14 ± 8.6[d]
3c	OCH_3	Pr	34.70 ± 1.32[d]	96.43 ± 10.6[d]
3d	OCH_3	Bu	49.76 ± 1.53[d]	120.50 ± 12.3[d]
3e	OCH_3	c-C_3H_5	62.24 ± 4.68[d]	123.35 ± 11.1[d]
3f	OCH_3	c-C_4H_7	38.30 ± 3.33[d]	96.54 ± 9.07[d]
3g	OCH_3	c-C_5H_9	49.87 ± 4.13[d]	105.19 ± 10.1[d]
3h	OCH_3	c-C_6H_3	62.20 ± 1.91[d]	87.36 ± 7.9[d]
3i	OCH_3	Ph	58.92 ± 3.55[d]	e
3j	H	Me	33.69 ± 3.62[d]	77.85 ± 8.6[d]
3k	H	Et	36.47 ± 4.52[d]	85.25 ± 7.8[d]
3l	H	Pr	52.39 ± 2.24[d]	84.95 ± 7.9[d]
3m	H	c-C_3H_5	38.79 ± 3.18[d]	86.93 ± 9.4[d]
3n	H	Ph	57.05 ± 3.13[d]	82.46 ± 9.9[d]
3o	Cl	Me	47.58 ± 4.01[d]	110.59 ± 10.5[d]
3p	Cl	Et	46.15 ± 5.66[d]	97.74 ± 11.1[d]
3q	Cl	Pr	34.43 ± 3.70[d]	97.74 ± 10.2[d]
3r	Cl	c-C_3H_5	70.24 ± 5.60[d]	98.12 ± 10.1[d]
3s	Cl	Ph	61.12 ± 3.30[d]	105.71 ± 9.5[d]
4a	OCH_3	Me	65.36 ± 5.60	101.52
4b	OCH_3	Et	50.87 ± 4.36	99.37
4c	OCH_3	Pr	42.82 ± 4.00	e
4d	OCH_3	Bu	39.65 ± 2.59	97.19
4e	OCH_3	c-C_3H_5	40.41 ± 4.27	99.89
4f	OCH_3	c-C_4H_7	33.73 ± 2.98	92.22
4g	OCH_3	c-C_5H_9	45.04 ± 4.45	96.34
4h	OCH_3	c-C_6H_{11}	48.24 ± 4.90	99.64
4i	OCH_3	C_6H_5	46.46 ± 4.46	97.23
4j	Cl	Me	31.69 ± 1.13	e
4k	Cl	c-C_3H_5	23.28 ± 3.54	e
4l	Cl	C_6H_5	21.71 ± 2.60	e

[a] Data represent the mean $\pm$ SEM of the percentage of nNOS inhibition produced by 1 mM concentration of each compound. Each value is the mean of three experiments performed by triplicate in homogenates of four rat striata in each one. *[b]* Data represent the mean $\pm$ SEM of the KYN3OH activity in the presence of 1 mM concentration of each compound. *[c]* See ref 23. *[d]* See ref 24. *[e]* Not tested.

Kynurenines **2a** and **2b** have also been tested as inhibitors of the kynurenine 3-hydroxylase (KYN3OH).[24] The most interesting result from these experiments was that **2a** and **2b** showed no inhibitory activity against this enzyme. Because both compounds are able to inhibit both the NMDA-dependent excitability and nNOS activity, we concluded that their inhibitory properties are due to the nNOS inhibition.

2a and **2b** bear a 2′-NH_2 group on the benzene ring, and this feature seems to be necessary for the nNOS inhibition because the removal of this group caused a significant decrease in the inhibitory response. The 2′-NH_2 group can condition the inhibitory activity in two different ways: (i) by restricting the conformational mobility of the kynurenine side chain and, hence, allowing the side chain to mimic melatonin, a known nNOS inhibitor, and (ii) by forming an additional hydrogen bond with some critical residues of nNOS when the complex is formed.

4,5-Dihydro-*1H*-pyrazole derivatives **3** were designed as more rigid nNOS inhibitors bearing the pharmacophoric features of kynurenines **2**.[24] These molecules bear the 2′-NH_2 group that forms the intramolecular hydrogen bond with the N-2 pyrazole atom and can also
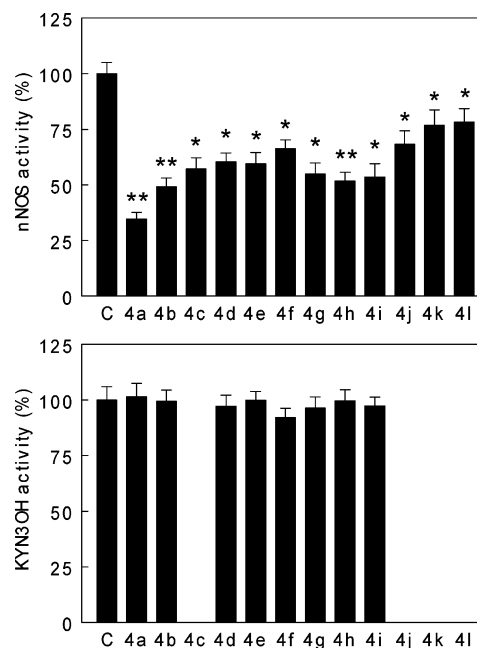

Figure 1. Percent of nNOS (top) and KYN3OH (bottom) activities in the presence of a 1 mM concentration of each compound as compared with those of untreated samples (C). Each value is the mean of three experiments performed by triplicate in homogenates of four rat striata in each one. *$P <$ 0.01 and **$P <$ 0.001 vs control.

produce a favorable interaction with the enzyme. On the other hand, the pyrazole ring confers rigidity to the molecule, and the final amide moiety can act in a way similar to that of the amide group of kynurenines **2**. We have found that compounds **3** show good nNOS inhibition, depending on the nature of both R_1 and R_2 substituents. Even more, compounds **3** are inactive against KYN3OH, indicating that their potential neuroprotective properties are due again to the nNOS inhibition.

From the comparison of kynurenines **2** and dihydropyrazoles **3**, a pharmacophore model (Figure 3) for the interaction with nNOS has been developed.[24] This model includes the aromatic ring, the 2′-NH_2 group, and the terminal amide CO fragment and can explain the structure−activity relationships for both families of compounds. Briefly, the model for the interaction includes: (i) a pocket in the enzyme that accommodates the benzene rings (red arc); (ii) a hydrogen-bond acceptor residue for the interaction with the free NH bond of the 2′-NH_2 group (blue arrow). (iii) a hydrogen-bond donor residue that can interact with the amide oxygen atom of both kynurenine and pyrazole derivatives (red arrow), and (iv) two different zones near the binding pocket that accommodates the R_2 substituent of kynurenines **2** and pyrazolines **3**. Because an increment in the R_2 volume in kynurenines provokes a decrease in activity, these molecules must orientate the R_2 substituent to a region with a small steric tolerance. On the contrary, the R_2 substituent in pyrazolines must be orientated to a zone sterically allowed.

Conformational analysis of kynurenamines **4** indicates a behavior similar to that of kynurenines **2**. Molecular modeling studies were performed using the Sybyl software[27] running on a Silicon Graphics workstation. Three-dimensional models of all compounds

Rel. E. = 3.94 kcal/mol   Rel. E. = 0.00 kcal/mol

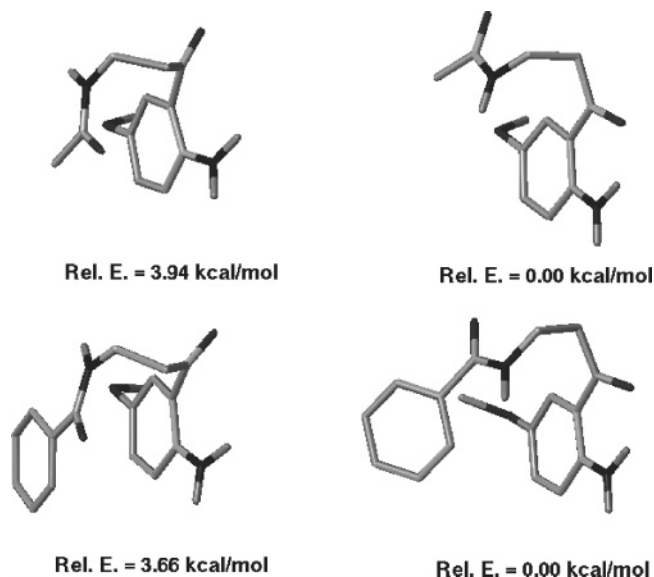Rel. E. = 3.66 kcal/mol   Rel. E. = 0.00 kcal/mol

Figure 2. Two more-stable conformations belonging to family I (left) and II (right) for **4a** (up) and **4i** (down). Only polar hydrogen atoms are shown for clarity. Relative energies (kcal/mol) are defined in relation to the most stable conformer found. In **4i**, the $\pi-\pi$ stacking interaction can be observed

were built from a standard fragment library, and their geometries were subsequently optimized using the Tripos force field[28] including the electrostatic term calculated from Gasteiger and Hückel[29] charges ($\epsilon = 1$, distance dependent). The method of Powell[30] included in the Maximin2 procedure was used for energy minimization until the gradient value was smaller than 0.01 kcal/mol·Å^2.

After the initial optimization, a conformational search of each compound using the Sybyl Gridsearch utility has been performed to locate the most stable conformer. With this purpose, all side-chain rotatable bonds have been rotated using an interval of 60°; the resulting conformations have been optimized after the elimination of all the constraints. The comparison of all of the optimized conformers to each other allows us to identify those that are energetically and geometrically unique.

Two main conformational families could be identified depending on the orientation of the carbonyl group; in one of them (type I), the oxygen atom points toward the methoxy group, and in the other (type II), it is orientated in the opposite direction, toward the 2'-NH$_2$ group. Figure 2 shows as an example the most stable conformer of each type of family for **4a**, the metabolite of melatonin.

In general, conformations of family II are stabilized by the formation of an intramolecular hydrogen bond between the CO and the NH$_2$ moieties, whereas conformations belonging to family I are more energetic.

For **4a**−**i**, there exists a higher number of conformations due to the existence of rotamers around the C−OMe bond. **4c** (R$_2$ = Pr) and **4d** (R$_2$ = Bu) have not been studied due to the high number of conformations expected (46.656 and 279.936, respectively), but the conformational behavior must be similar to that of the analogues with smaller side chains.

The comparison of all conformers of kynurenamines **4** with those of pyrazolines **3** using the benzene ring, the 2'-NH$_2$ group, and the oxygen atom of the amide

terminal group demonstrates that a low-energy conformation of kynurenamines can be superimposed on our pharmacophore model in a way similar to that of kynurenines.

Table 2 shows some data of the conformational behavior of these compounds, among them the total number of conformers, the range of relative energies comprising all conformations, the relative energy of the most stable conformer of each family, and the relative energy of the conformation that matches the pharmacophore model.

The active conformation belongs in all cases to the family II of conformations and in general is more stable than the preferred type I conformation. Only in **4i** and **4l** is the energy of the pharmacophoric conformation higher, but it could be due to an additional stabilization of conformations type I and II due to a $\pi-\pi$ stacking interaction between both benzene moieties (Figure 2).

Figure 3 shows as an example the superposition of **4a** and **3a**. It can be observed that the benzene ring, the 2'-NH$_2$ group, and the terminal amide oxygen atom coincide very well (RMSD = 0.53 Å). Furthermore, the energy of this conformation of **4a** is only 2.75 kcal/mol, a value that can be easily compensated by the enzyme−ligand interaction. In general, all studied compounds match the pharmacophore with conformations of low energy (Table 2).

This superimposition shows that the R$_2$ substituent in kynurenamines **4** is orientated in a way similar to that in kynurenines **2**, that is toward the more hindered zone of the interaction model, and this orientation justifies the fact that the inhibition activity decreases when the volume of R$_2$ increases. In kynurenamines **4**, the influence of R$_2$ over the biological activity is even clearer than in kynurenines, because only two derivatives (**2a** and **2b**) were synthesized and tested in this family, whereas 12 kinurenamines (**4a-4l**) have been prepared. The influence of an increment of R$_2$ volume is also independent of the R$_1$ nature, and consequently, the structure−activity relationships found for kynurenamines **4** confirm our model for the interaction with nNOS.

The comparison of the activity of kynurenines **2a** and **2b** with that of their corresponding kynurenamine derivatives **4a** and **4c** (Table 1) indicates a slightly higher inhibition activity for compounds of type **2**. Nevertheless, the differences in activity are not high enough to consider that kynurenines are more potent as nNOS inhibitors.

Conclusions

Kynurenamines **4** show good nNOS inhibition, showing structure−activity relationships similar to those of kynurenines **2**, and as a whole, pyrazoline derivatives **3** are better nNOS inhibitors than **2** or **4**. Our pharmacophore model fulfills all of the SARs for the three families of compounds and supports the results obtained in the kynurenamine family. Among these compounds, the melatonin metabolite aMK (**4a**) is the more-potent nNOS inhibitor.

Experimental Section

Melting points were determined using an Electrothermal-1A-6301 apparatus and are uncorrected. ^{1}H NMR and ^{13}C NMR spectra were recorded on a Bruker AMX 300 spectrom-
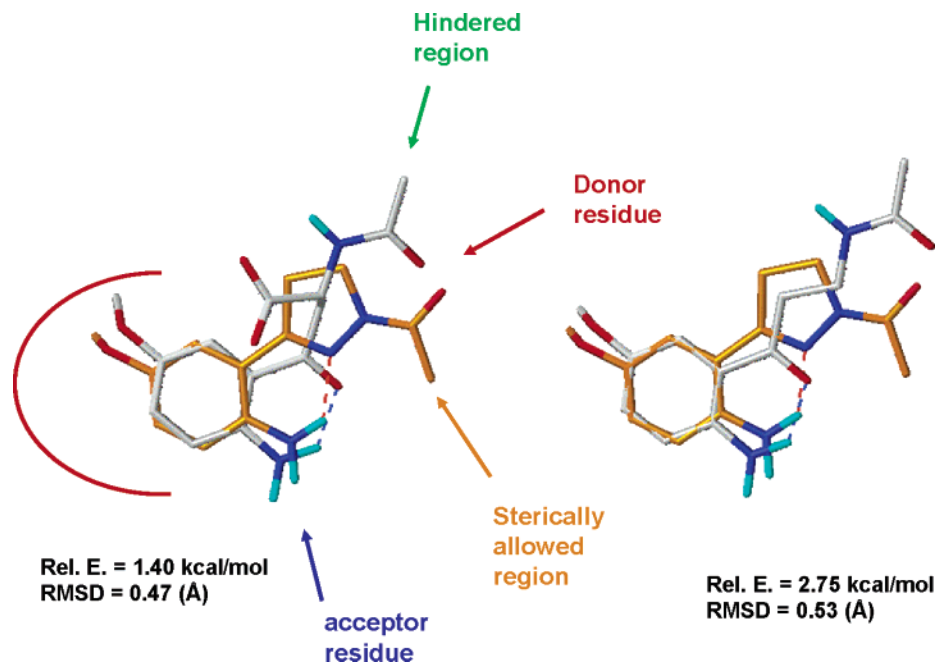
Figure 3. (left) Pharmacophore model for the inhibition of nNOS defined by the superimposition of **2a** (colored by atoms) and **3a** (carbon atoms colored in orange). (Right) The same superposition for the corresponding conformations of **4a** and **3a**. Relative energies correspond to the **2a** or **4a** conformation, and RMSD indicates the goodness of the superimposition considering the aromatic ring, the 2′-NH$_2$ group, and the amide oxygen atom as fitting atoms. Red arc indicates the hydrophobic pocket of the benzene ring. Blue and red arrows indicate the interaction with the hydrogen-bond acceptor and donor residues, respectively. Pockets for allocation of the R$_2$ amide substituent are indicated by the green (kynurenines and kinurenamines) and orange (pyrazoles) arrows. Similar orientation of R$_2$ in **2** and **4** justifies the observed structure−activity relationships.

Table 2. Some Data of the Conformational Behavior of **4a,b** and **4e−l**

cmpd	no. of conformers found	rel E^a range	more stable type I conformer rel E^a	more stable type II conformer rel E^a	active conformation rel E^a
4a	297	0.00−15.29	3.94	0.00	2.75
4b	1036	0.00−17.50	4.81	0.00	2.96
4e	463	0.00−12.57	4.54	0.00	3.45
4f	492	0.00−12.57	4.87	0.00	3.98
4g	476	0.00−16.67	5.10	0.00	3.40
4h	369	0.00−13.08	4.22	0.00	3.74
4i	713	0.00−14.15	3.66	0.00	5.16
4j	73	0.00−10.29	3.97	0.00	2.45
4k	116	0.00−10.12	3.77	0.00	2.58
4l	101	0.00−12.11	3.22	0.00	4.50

^{a} Relative energies (kcal/mol) defined in relation to the most stable conformer found for each compound.

eter operating at 75.479 MHz for ^{13}C NMR and 300.160 MHz for ^{1}H in CDCl$_3$ and on a Bruker ARX 400 spectrometer operating at 400.132 MHz for ^{1}H and 100.623 MHz for ^{13}C (at concentration of ca. 27 mg mL^{-1} in all cases). The center of each peak of CDCl$_3$ [7.26 ppm (^{1}H) and 77.0 ppm (^{13}C)] was used as the internal reference in a 5 mm ^{13}C/^{1}H dual probe (Wilmad, No. 528-PP). The temperature of the sample was maintained at 297 K. The peaks are reported in ppm (%). High-resolution mass spectroscopy (HRMS) was carried out on a VG AutoSpec Q high-resolution mass spectrometer (Fisons Instruments). Elemental analyses were performed on a Perkin-Elmer 240 C and agreed with theoretical values within 0.4%. Flash chromatography was carried out using silica gel 60 and 230−240 mesh (Merck), and the solvent mixture reported in parentheses was used as eluent.

Preparation of *N*-[3-(2-Nitro-5-substituted-phenyl)-3-oxopropyl]phthalimide 6a,b. General Method. α,β-Unsaturated ketone[25] **5a,b** (9.61 mmol) was added to a mixture of phthalimide (1.781 g, 9.61 mmol) and sodium methoxyde (0.01 g, 0.20 mmol) dissolved in DMSO (20 mL). The mixture was stirred at room temperature for 2 h and then slowly diluted with 30 mL of water. The resultant slurry was filtered, washed with water, and dried to give a white, crystalline solid.

***N*-[3-(5-Methoxy-2-nitrophenyl)-3-oxopropyl]phthalimide, 6a:** (90%); mp 173−176 °C; MS (LSIMS): *m/z* 377.074931 (M + Na)$^+$, calcd mass for C$_{18}$H$_{14}$N$_2$O$_6$Na: 377.074956 (deviation 0.1 ppm).

***N*-[3-(5-Chloro-2-nitrophenyl)-3-oxopropyl]phthtalimide, 6b:** (92%); mp 178−180 °C; MS (LSIMS): *m/z* 381.025490 (M + Na)$^+$, calcd mass for C$_{17}$H$_{11}$ClN$_2$O$_5$Na: 381.025419 (deviation −0.2 ppm).

Preparation of *N*-[3,3-Ethylenedioxy-3-(2-nitro-5-substitutedphenyl)propyl]phthalimide, 7a,b. General Method. A mixture of the β-phthalimido ketone **6a,b** (11 mmol), ethylene glycol (3.5 mL), and *p*-toluenesulfonic acid (0.17 g) in toluene (16 mL) was refluxed using a Dean−Stark trap for 10 h. The cooled mixture was washed with saturated aqueous sodium bicarbonate and saturated brine, dried over anhydrous magnesium sulfate, filtered, and evaporated to yield the crude product, which was purified by flash chromatography (ether−hexane, 1:3).

***N*-[3,3-Ethylenedioxy-3-(5-methoxy-2-nitrophenyl)propyl]phthalimide 7a:** (85%); mp 134−137 °C; MS (LSIMS): *m/z* 421.101027 (M + Na)$^+$, calcd mass for C$_{20}$H$_{18}$N$_2$O$_7$Na: 421.101171 (deviation 0.3 ppm).

***N*-[3,3-Ethylenedioxy-3-(5-chloro-2-nitrophenyl)propyl]phthalimide, 7b:** (85%); mp 134−136 °C; MS (LSIMS):

m/z 425.052029 (M + Na)$^+$, calcd mass for $C_{19}H_{15}ClN_2O_6Na$: 425.051634 (deviation −0.9 ppm).

Preparation of *N*-[3-(2-Nitrophenyl-5-substituted)-3-oxopropyl]alquil-amides, 10a−l. General Method. To a solution of 0.69 mmol of the corresponding phthalimide **7a,b** in 20 mL of dry ethanol was added 0.1 mL (2.07 mmol) of 95% hydrazine. The mixture was heated at reflux for 4.5 h and then made acidic (pH ≥ 2) with concentrated hydrochloric acid. Heating was continued for an additional hour, and after cooling, the resulting suspension was removed by filtration. The filtrate was diluted with an equal volume of water and then washed with ether. The ether washings were discarded, and the aqueous layer was rendered alkaline (pH ≥ 10) with solid potassium hydroxide. Extraction with ether (2 × 25 mL), combination of the ethereal fractions, drying (Na_2SO_4), filtration, and concentration gave the amine, which was dissolved in CH_2Cl_2. Then, Et_3N (slight molar excess) and acetic anhydride or the corresponding acyl chloride (1 mol equiv) in CH_2Cl_2 were added dropwise with stirring at room temperature. This solution was stirred for 3 h. The resulting solid was filtered and washed with H_2O, 10% aqueous HCl, 2 M NaOH, H_2O, and brine. The filtrate was then dried (Na_2SO_4) and filtered, and the solvent was removed under reduced pressure. Flash chromatography (ether/hexane, 1:4) afforded the acyl derivative.

***N*-[3-(5-Methoxy-2-nitrophenyl)-3-oxopropyl]acet-amide, 10a:** (70%); mp 96−99 °C; MS (LSIMS): *m/z* 289.079559 (M + Na)$^+$, calcd mass for $C_{12}H_{14}N_2O_5Na$: 289.080041 (deviation 1.7 ppm).

***N*-[3-(5-Methoxy-2-nitrophenyl)-3-oxopropyl]propion-amide, 10b:** (70%); mp 91−94 °C; MS (LSIMS): *m/z* 303.095641 (M + Na)$^+$, calcd mass for $C_{13}H_{16}N_2O_5Na$: 303.095692 (deviation 0.2 ppm).

***N*-[3-(5-Methoxy-2-nitrophenyl)-3-oxopropyl]butir-amide, 10c:** (75%); mp 120−123 °C; MS (LSIMS): *m/z* 317.111261 (M + Na)$^+$, calcd mass for $C_{14}H_{18}N_2O_5Na$: 317.111342 (deviation 0.3 ppm).

***N*-[3-(5-Methoxy-2-nitrophenyl)-3-oxopropyl]pentan-amide, 10d:** (80%); mp 102−105 °C; MS (LSIMS): *m/z* 331.127409 (M + Na)$^+$, calcd mass for $C_{15}H_{20}N_2O_5Na$: 331.126992 (deviation −1.3 ppm).

***N*-[3-(5-Methoxy-2-nitrophenyl)-3-oxopropyl]cyclopro-panecarboxamide, 10e:** (85%); mp 146−149 °C; MS (LSIMS): *m/z* 293.113928 (M + H)$^+$, calcd mass for $C_{14}H_{17}N_2O_5$: 293.113747 (deviation −0.6 ppm).

***N*-[3-(5-Methoxy-2-nitrophenyl)-3-oxopropyl]cyclobu-tanecarboxamide, 10f:** (85%); mp 121−125 °C; MS (LSIMS): *m/z* 329.111172 (M + Na)$^+$, calcd mass for $C_{15}H_{18}N_2O_5Na$: 329.111342 (deviation 0.5 ppm).

***N*-[3-(5-Methoxy-2-nitrophenyl)-3-oxopropyl]cyclopen-tanecarboxamide, 10g:** (70%); mp 127−130 °C; MS (LSIMS): *m/z* 343.126051 (M + Na)$^+$, calcd mass for $C_{16}H_{20}N_2O_5Na$: 343.126992 (deviation 2.7 ppm).

***N*-[3-(5-Methoxy-2-nitrophenyl)-3-oxopropyl]cyclohex-anecarboxamide, 10h:** (75%); mp 155−157 °C; MS (LSIMS): *m/z* 357.143088 (M + Na)$^+$, calcd mass for $C_{17}H_{22}N_2O_5Na$: 357.142642 (deviation −1.2 ppm).

***N*-[3-(5-Methoxy-2-nitrophenyl)-3-oxopropyl]benz-amide, 10i:** (70%); mp 127−130 °C; MS (LSIMS): *m/z* 351.095991 (M + Na)$^+$, calcd mass for $C_{17}H_{16}N_2O_5Na$: 351.095692 (deviation −0.9 ppm).

***N*-[3-(5-Chloro-2-nitrophenyl)-3-oxopropyl]acet-amide, 10j:** (83%); mp 118−120 °C; MS (LSIMS): *m/z* 293.030872 (M + Na)$^+$, calcd mass for $C_{11}H_{11}ClN_2O_4Na$: 293.030504 (deviation −1.3 ppm).

***N*-[3-(5-Chloro-2-nitrophenyl)-3-oxopropyl]cyclopro-panecarboxamide, 10k:** (85%); mp 153−156 °C; MS (LSIMS): *m/z* 319.046468 (M + Na)$^+$, calcd mass for $C_{13}H_{13}ClN_2O_4Na$: 319.046155 (deviation −1.0 ppm).

***N*-[3-(5-Chloro-2-nitrophenyl)-3-oxopropyl]benz-amide, 10l:** (90%); mp 146−148 °C; MS (LSIMS): *m/z* 355.045920 (M + Na)$^+$, calcd mass for $C_{16}H_{13}ClN_2O_4Na$: 355.046155 (deviation 0.7 ppm).

Preparation of *N*-[3-(2-Amino-5-methoxyphenyl)-3-oxopropyl]alquilamides, 4a-4i. General Method. A mixture of nitroarene **10a−i** (0.414 mmol), palladium/carbon (10%, 10 mg), and methanol (20 mL) was stirred at room temperature under a hydrogen atmosphere (1 atm). After 3 h, the suspension was filtered through Celite and evaporated. The residue was dissolved in CH_2Cl_2, and this solution was washed with water, dried over magnesium sulfate, filtered, and concentrated. The resulting yellow solid was recrystallized from CH_2Cl_2/hexane to afford the corresponding aromatic amine with quantitative yield.

***N*-[3-(2-Amino-5-methoxyphenyl)-3-oxopropyl]acet-amide, 4a:** (100%); mp 88−91 °C; MS (LSIMS): *m/z* 259.105986 (M + Na)$^+$, calcd mass for $C_{12}H_{16}N_2O_3Na$: 259.105862 (deviation −0.5 ppm). Anal. $C_{12}H_{16}N_2O_3$ (C, H, N).

***N*-[3-(2-Amino-5-methoxyphenyl)-3-oxopropyl]propi-onamide, 4b:** (100%); mp 64−68 °C; MS (LSIMS): *m/z* 273.121551 (M + Na)$^+$, calcd mass for $C_{13}H_{18}N_2O_3Na$: 273.121512 (deviation −0.1 ppm). Anal. $C_{13}H_{18}N_2O_3$ (C, H, N).

***N*-[3-(2-Amino-5-methoxyphenyl)-3-oxopropyl]butir-amide, 4c:** (100%); mp 71−74 °C; MS (LSIMS): *m/z* 287.136678 (M + Na)$^+$, calcd mass for $C_{14}H_{20}N_2O_3Na$: 287.136888 (deviation 1.7 ppm). Anal. $C_{14}H_{20}N_2O_3$ (C, H, N).

***N*-[3-(2-Amino-5-methoxyphenyl)-3-oxopropyl]pentan-amide, 4d:** (100%); mp 82−86 °C; MS (LSIMS): *m/z* 301.152572 (M + Na)$^+$, calcd mass for $C_{15}H_{22}N_2O_3Na$: 301.152813 (deviation 0.8 ppm). Anal. $C_{15}H_{22}N_2O_3$ (C, H, N).

***N*-[3-(2-Amino-5-methoxyphenyl)-3-oxopropyl]cyclo-propanocarboxamide, 4e:** (100%); mp 103−108 °C; MS (LSIMS): *m/z* 285.121271 (M + Na)$^+$, calcd mass for $C_{14}H_{18}N_2O_3Na$: 285.121512 (deviation 0.8 ppm). Anal. $C_{14}H_{18}N_2O_3$ (C, H, N).

***N*-[3-(2-Amino-5-methoxyphenyl)-3-oxopropyl]cyclo-butanocarboxamide, 4f:** (100%); mp 98−102 °C; MS (LSIMS): *m/z* 299.137078 (M + Na)$^+$, calcd mass for $C_{15}H_{20}N_2O_3Na$: 299.137162 (deviation 0.3 ppm). Anal. $C_{15}H_{20}N_2O_3$ (C, H, N).

***N*-[3-(2-Amino-5-methoxyphenyl)-3-oxopropyl]cyclo-pentanocarboxamide, 4g:** (100%); mp 112−115 °C; MS (LSIMS): *m/z* 291.170685 (M + H)$^+$, calcd mass for $C_{16}H_{22}N_2O_3$: 291.170868 (deviation 0.6 ppm). Anal. $C_{16}H_{22}N_2O_3$ (C, H, N).

***N*-[3-(2-Amino-5-methoxyphenyl)-3-oxopropyl]cyclo-hexanocarboxamide, 4h:** (100%); mp 130−135 °C; MS (LSIMS): *m/z* 327.167893 (M + Na)$^+$, calcd mass for $C_{17}H_{24}N_2O_3Na$ 327.168188 (deviation 1.7 ppm). Anal. $C_{17}H_{24}N_2O_3$ (C, H, N).

***N*-[3-(2-amino-5-methoxyphenyl)-3-oxopropyl]benz-amide, 4i:** (100%); mp 112−115 °C; MS (LSIMS): *m/z* 321.121849 (M + Na)$^+$, calcd mass for $C_{17}H_{18}N_2O_3Na$: 321.121512 (deviation −1.0 ppm). Anal. $C_{17}H_{18}N_2O_3$ (C, H, N).

Preparation of *N*-[3-(2-Amino-5-chloro-phenhyl)-3-oxopropyl]alquilamides, 4j−l. General Method. To a suspension of the nitroarene **10j−l** (0.524 mml) in refluxing water was added Fe (0.29 g, 5.24 mmol) and $FeSO_4$ (0.15 g, 0.524 mmol). The reaction mixture was refluxed for 3 h, filtrated through Celite, and washed thoroughly with CH_2Cl_2. The aqueous phase was extracted with CH_2Cl_2 (3 × 15 mL) and EtOAc (3 × 15 mL). The organic layer was washed with brine, dried (Na_2SO_4), filtered, and evaporated. The crude mixture was purified by recrystallization from CH_2Cl_2/hexane.

***N*-[3-(2-Amino-5-chlorophenyl)-3-oxopropyl]acet-amide, 4j:** (95%); mp 116−118 °C; MS (LSIMS): *m/z* 263.056220 (M + Na)$^+$, calcd mass for $C_{11}H_{13}ClN_2O_2Na$: 263.056325 (deviation 0.4 ppm). Anal. $C_{11}H_{13}ClN_2O_2$ (C, H, N).

***N*-[3-(2-Amino-5-chlorophenyl)-3-oxopropyl]cyclopro-panocarboxamide, 4k:** (95%); mp 163−165 °C; MS (LSIMS): *m/z* 289.072317 (M + Na)$^+$, calcd mass for $C_{13}H_{15}ClN_2O_2Na$: 289.071975 (deviation −1.2 ppm). Anal. $C_{13}H_{15}ClN_2O_2$ (C, H, N).

***N*-[3-(2-Amino-5-chlorophenyl)-3-oxopropyl]benz-amide, 4l:** (95%); mp 149−151 °C; MS (LSIMS): *m/z* 325.072043 (M + Na)$^+$, calcd mass for $C_{16}H_{15}ClN_2O_2Na$: 325.071975 (deviation −0.2 ppm). Anal. $C_{16}H_{15}ClN_2O_2$ (C, H, N).

Striatal nNOS Activity Determination

L-Arginine, L-citruline, N-(2-hydroxymethyl)piperazine-N'-(2-ethanesulfonic acid) (HEPES), DL-dithiothreitol (DTT), leupeptin, aprotinin, pepstatin, phenylmethylsulfonylfluoride (PMSF), hypoxanthine-9-β-D-ribofuranosid (inosine), ethylene glycol-bis-(2-aminoethyl ether)-N,N,N',N'-tetraacetic acid (EGTA), bovine serum albumin (BSA), Dowex-50 W (50 × 8-200), FAD, NADPH, and 5,6,7,8-tetrahydro-L-biopterin dihydrocloride (H$_4$-biopterin) were obtained from Sigma-Aldrich Química (Spain). L-[^{3}H]-Arginine (58 Ci/mmol) was obtained from Amersham (Amersham Biosciences, Spain). Tris (hydroxymethyl)aminometane (Tris-HCl) and calcium chloride were obtained from Merck (Spain).

The rats were killed by cervical dislocation, and the striata were quickly collected and immediately used to measure NOS activity. Upon removal, the tissues were cooled in ice-cold homogenizing buffer (25 mM Tris, 0.5 mM DTT, 10 μg/mL leupeptin, 10 μg/mL pepstatin, 10 μg/mL aprotinine, and 1 mM PMSF at pH 7.6). Two striata were placed in 1.25 mL of the same buffer and homogenized in a Polytron (10 s × 6). The crude homogenate was centrifuged for 5 min at 1000g, and aliquots of the supernatant were either stored at −20 °C for total protein determination[31] or used immediately to measure NOS activity. The nNOS activity was measured by the Bredt and Snyder[32] method, monitoring the conversion of L-[^{3}H]-arginine to L-[^{3}H]-citruline. The final incubation volume was 100 μL and consisted of 10 μL of crude homogenate added to a buffer to give a final concentration of 25 mM Tris, 1 mM DTT, 30 μM H$_4$-biopterin, 10 μM FAD, 0.5 mM inosine, 0.5 mg/mL BSA, 0.1 mM CaCl$_2$, 10 μM L-arginine, and 50 nM L-[^{3}H]-arginine at pH 7.6. The reaction was started by the addition of 10 μL of NADPH (0.75 mM final) and 10 μL of each pyrazole derivative in DMSO to give a final concentration of 1 mM. The tubes were vortexed and incubated at 37 °C for 30 min. Control incubations were performed by the omission of NADPH. The reaction was halted by the addition of 400 μL of cold 0.1 M HEPES, 10 mM EGTA, and 0.175 mg/mL L-citruline at pH 5.5. The reaction mixture was decanted into a 2-mL column packet with Dowex-50 W ion-exchange resin (Na$^+$ form) and eluted with 1.2 mL of water. L-[^{3}H]-Citruline was quantified by liquid scintillation spectroscopy. The retention of L-[^{3}H]-arginine in this process was greater than 98%. Specific enzyme activity was determined by subtracting the control value, which usually amounted to less than 1% of the radioactivity added. The nNOS activity was expressed as pmol of L-[^{3}H]-citruline produced (mg of protein)$^{-1}$ min^{-1}.

Striatal KYN3OH Activity Determination

L-Kynurenine, 3-hydroxykynurenine, sucrose, NADPH, DHBA, DMSO, perchloric acid, triethylamine, phosphoric acid, heptanesulfonic acid, and EDTA-Na$_2$ were obtained from Sigma-Aldrich (Spain). HPLC-grade acetonitrile was obtained from Panreac (Spain). The water used for the preparation of solutions was of Milli-RO/Q grade (Millipore Iberica, Spain). All remaining chemicals were of analytical grade and were purchased from Sigma-Aldrich (Spain).

Tissue for KYN3OH determination was prepared from rats killed by cervical dislocation. Striata were rapidly removed, washed in cold saline, homogenized in 8 vol of sucrose (0.31 M), and centrifuged at 10 000g for 30 min at 4 °C. The pellets were rinsed in sucrose (0.32 M) and centrifuged twice. The obtained pellets were resuspended in 8 vol of 0.14 M KCl and 20 mM phosphate buffer at pH 7 and frozen to −20 °C until the assay.

The KYN3OH activity was measured following the Carpenedo[33] method, monitoring the conversion of L-kynurenine to 3-hydroxykynurenine. The final incubation volume was 120 μL and consisted in 100 μL of crude homogenate added to the buffer to give a final concentration of 0.1 M phosphate, 4 mM MgCl$_2$, and 100 μM L-kynurenine. This solution was completed with 10 μL of 40 mM NADPH and 10 μL of each pyrazole derivative at a final concentration of 1 mM in DMSO. The tubes were vortexed and incubated at 37 °C for 60 min. The reaction was stopped, the tubes were placed on ice, and 100 μL of cold 1 M perchloric acid was added. To this mixture was added 10 μL DHBA as internal standard, and the samples were centrifuged at 12 000g for 10 min at 4 °C. The supernatant was removed and frozen to −20 °C until 3-hydroxykynurenine determination. The concentration of 3-hydroxykynurenine was quantified by HPLC with electrochemical detection, following the method of Heyes and Quearry[34] with slight modifications. Separation was done in a C-18 reversed-phase 3-μm sphere analytical column. The applied potential was set at +0.6 V using a glass carbon electrode versus an Ag/AgCl reference electrode. The mobile phase consisted of 20 mL of acetonitrile, 9 mL of triethylamine, 5.9 mL of phosphoric acid, 100 mg of EDTA-Na$_2$, and 1.8 g of heptanesulfonic acid in 1000 mL of deionized water. The solution was filtered through a 0.45-μm filter and degassed before use. Analyses were done at a flow rate of 1 mL/min at room temperature. The concentration of 3-hydroxykynurenine was calculated using DHBA as the internal standard and a calibration curve obtained from the corresponding standard injected in the HPLC system. The calculated concentration is expressed as nmol/h/g wet brain.

Statistical Analysis

Data are expressed as the mean ± SEM. One-way analysis of variance, followed by the Newman−Keuls multiple range test, was used. A $P < 0.05$ value was considered statistically significant.

Supporting Information Available: Spectroscopic data (¹H and ¹³C NMR) of **4a−l**, **5a−b**, **6a−b**, and **10a−l** and elemental analyses data for **4a−l**. This material is available free of charge via the Internet at http://pubs.acs.org.

References

(1) Dingledine, R.; Borges, K.; Bowie, D.; Traynelis, S. F. The glutamate receptor ion channels. *Pharmacol. Rev.* **1999**, *51*, 7−61.
(2) Herrling, P. L. Clinical implications of NMDA receptors. In *The NMDA Receptor*; Colingridge, G. L., Watkins, J. C., Eds.; Oxford University Press: Oxford, 1994; pp 376−394.
(3) Meldrum, B.; Garthwaite, J. Excitatory amino acid neurotoxicity and neurodegenerative diseases. *Trends Pharmacol. Sci.* **1990**, *11*, 379−387.

(4) Sattler, R.; Tymianski, M. Molecular mechanisms of calcium dependent excitotoxicity. *J. Mol. Med.* **2000**, *78*, 3−13.

(5) Moncada, S.; Palmer, R. M. J.; Higgs, E. A. Nitric Oxide: Physiology, Pathophysiology, and Pharmacology. *Pharmacol. Rev.* **1991**, *43*, 109−142.

(6) Mayer, B. M.; John, M.; Bohme, E. Purification of a Ca^{2+}/Calmodulin-Dependent Nitric Oxide Synthase from Porcine Cerebellum: Cofactor Role of Tetrahydrobiopterin. *FEBS Lett.* **1990**, *277*, 215−219.

(7) Pollock, J. S.; Förstermann, U.; Mitchel, J. A.; Warner, T. D.; Schmidt, H. H.; Nakane, M.; Murad, F. Purification and Characterization of Particulate Endothelium Derived Relaxing Factor Synthase from Cultured and Native Bovine Aortic Endothelial Cells. *Proc. Natl. Acad. Sci. U.S.A.* **1991**, *88*, 10480−10484.

(8) Stuehr, D. J.; Cho, H. J.; Kwon, N. S.; Weise, M. F.; Nathan, C. F. Purification and Characterization of the Cytokine-Induced Macrophage Nitric Oxide Synthase: A FAD-Containing and FMN-Containing Flavoproteins. *Proc. Natl. Acad. Sci. U.S.A.* **1991**, *88*, 7773−7777.

(9) Hevel, J. M.; White, K. A.; Marletta, M. A. Purification of the Inducible Murine Macrophage Nitric Oxide Synthase. Identification as a Flavoprotein. *J. Biol. Chem.* **1991**, *266*, 22789−22791.

(10) Knowles, R. G.; Palacios, M.; Palmer, M. R. J.; Moncada, S. Formation of Nitric Oxide from L-Arginine in the Central Nervous System: A Transduction Mechanism for Stimulation of the Soluble Guanylate Cyclase. *Proc. Natl. Acad. Sci. U.S.A.* **1989**, *86*, 5159−5162.

(11) McCall, T. B.; Boughton-Smith, N. K.; Palmer, R. M. J.; Whittle, B. J. R.; Moncada, S. Synthesis of Nitric Oxide from L-arginine by Neutrophils: Release and Interaction with Superoxide Anion. *Biochem. J.* **1989**, *261*, 293−296.

(12) Pozo, D.; Osuna, C.; Calvo, J. R.; Guerrero, J. M.: Producción de Oxido Nítrico y su Modulacion en el Sistema Inmune y el Sistema Nervioso. *Arch. Neurocienc.* **1998**, *3*, 84−94.

(13) Smith, M. A.; Vasak, M.; Knipp, M.; Castellani, R. J.; Perry, G. Dimethylargininase, a nitric oxide protein, in Alzheimer disease. *Free Radical Biol. Med.* **1998**, *25*, 898−902.

(14) Yew, D. T.; Wong, H. W.; Li, W. P.; Lai, H. W.; Yu, W. H. Nitric oxide synthase in different areas of normal aged and Alzheimer's brains. *Neuroscience* **1999**, *89*, 675−686.

(15) Wong, N. K.; Strong, M. J. Nitric oxide synthase expression in cervical spinal cord in sporadic amyotrophic lateral sclerosis. *Eur. J. Cell. Biol.* **1998**, *77*, 338−343.

(16) Norris, P. J.; Waldvogel, H. J.; Faull, R. L.; Love, D. R.; Emson, P. C. Decreased neuronal nitric oxide synthase messenger RNA and somatostatin messenger RNA in the striatum of Huntington's disease. *Neuroscience* **1996**, *4*, 1037−1047.

(17) León, J.; Vives, F.; Crespo, E.; Camacho, E.; Espinosa, A.; Gallo, M. A.; Escames, G.; Acuña-Castroviejo, D. Modification of Nitric Oxide Synthase Activity and Neuronal Response in Rat Striatum by Melatonin and Kynurenine Derivates. *J. Neuroendocrinol.* **1998**, *10*, 297−302.

(18) Escames, G.; León, J.; López, L. C.; Acuña-Castroviejo, D. Mechanisms of N-methyl-D-aspartate Receptor Inhibition by Melatonin In the Rat Striatum *J. Neuroendocrinol.* **2004**, *16*, 929−935.

(19) Cazevieille, C.; Safa, R.; Osborne, N. N. Melatonin protects primary cultures of rat cortical neurones from NMDA excito-

(20) Fujiwara, M.; Shibata, M.; Watanabe, Y.; Nukiwa, T.; Hirata, F.; Mizuno, N.; Hayaishi, O. Indoleamine 2,3-dioxygenase. Formation of L-kynurenine from L-tryptophan in cultured rabbit pineal gland *J. Biol. Chem.* **1978**, *253*, 6081−6087

(21) Hirata, F.; Hayaishi, O.; Tokuyama, T.; Seno, S. In vitro and in vivo formation of two new metabolites of melatonin. *J. Biol. Chem.* **1974**, *249*, 1311−1313.

(22) Kennaway, D. J.; Hugel, H. M. Melatonin binding sites: are they receptors? *Mol. Cell. Endocrinol.* **1992**, *88*, C1−9.

(23) Camacho, M. E.; León, J.; Carrión, M. D.; Entrena, A.; Escames, G.; Khaldy, H.; Acuña-Castroviejo, D.; Gallo, M. A.; Espinosa, A. Inhibition of nNOS Activity in Rat Brain by Synthetic Kynurenines: Structure−Activity Dependence. *J. Med. Chem.* **2002**, *45*, 263−274.

(24) Camacho, M. E.; León, J.; Entrena, A.; Velasco, G.; Carrión, M. D.; Escames, G.; Vivo, A.; Acuña-Castroviejo, D.; Gallo, M. A.; Espinosa, A. 4,5-Dihydro-*1H*-pyrazole Derivatives with Inhibitory nNOS Activity in Rat Brain: Synthesis and Structure−Activity Relationships *J. Med. Chem.* **2004**, *47*, 5641−5650.

(25) Hammen, P. D.; Braisted, A. C.; Northrup, D. L. Synthesis of vinyl and β-phthalimido ketones. *Synth. Commun.* **1991**, *21(21)*, 2157−2163.

(26) (a) Stone, T. W. Kynurenic acid antagonists and kynurenine pathway inhibitors. *Expert Opin. Invest.* Drugs **2001**, *10*, 633−645. (b) Stone, T. W. Kynurenines in the CNS: from endogenous obscurity to therapeutic importance. *Prog. Neurobiol.* **2001**, *64*, 185−218.

(27) SYBYL Molecular Modelling Software; Tripos Inc.: St. Louis, MO 63144-2913; www.tripos.com.

(28) Clark, M.; Cramer, R. D., III; Van Opdenbosch, N. Validation of the General Purpose Tripos 5.2 Force Field. *J. Comput. Chem.* **1989**, *10*, 982−1012.

(29) (a) Gasteiger, J.; Marsili, M. *Tetrahedron* **1980**, *36*, 3219−3228. (b) Marsili, M.; Gasteiger, J. *Croat. Chem. Acta* **1980**, *53*, 601−614. (c) Gasteiger, J.; Marsili, M. *Org. Magn. Reson.* **1981**, *15*, 353−360.

(30) Powell, M. J. D. Restart Procedures for Conjugate Gradient Method. *Math. Prog.* **1977**, *12*, 241−254.

(31) Lowry, O. H.; Rosebrough N. J.; Farr, A. S.; Randall, R. J. Protein measurement with the Folin phenol reagent. *J. Biol. Chem.* **1951**, *193*, 265−267.

(32) Bredt, D. S.; Snyder, S. H. Isolation of Nitric Oxide Synthethase, a Calmodulin Requiring Enzyme. *Proc. Natl. Acad. Sci. U.S.A.* **1990**, *87*, 682−685

(33) Carpenedo, R.; Chiarugi, A.; Russi, P.; Lombardi, G.; Carla, V.; Pellicciari, R.; Mattoli, L.; Moroni, F. Inhibitors of kynurenine hydroxylase and kynureninase increase cerebral formation of kynurenate and have sedative and anticonvulsant activities. *Neuroscience* **1994**, *61*, 237−243.

(34) Heyes, M. P.; Quearry, B. J. Quantification of 3-hydroxykynurenine in brain by high-perfomance liquid chromatography and electrochemical detection. *J. Chromatogr.* **1988**, *428*, 340−344.

toxicity and hypoxia/reoxygenation. *Brain Res.* **1997**, *768*, 120−124.